Renewable Energy Resource Risk Quantification and Mitigation Assessment for Mining Micro-Grid

Moksadur Rahman Stefan Thorburn

ABB Corporate Research Center, Forskargränd 7, 72226 Vasteras, Sweden

Abstract: As one of the most energy-intensive industries, mining accounts for over one-third of industrial final energy consumption. With the growing mineral demand, combined with declining ore grades, it is expected that the energy demand in mining will only grow in the future, potentially increasing its already large greenhouse gas footprint. With rising energy costs, renewable energy presents a viable option not only to improve the environmental footprint but also to reduce overall costs with optimized operation of mines. While renewable energy generators i.e., solar photovoltaics and wind turbines offer numerous benefits like modularity, environmentally friendliness, and natural availability; the major drawbacks are their temporal intermittency and seasonal and long-term variability. Hence, these generators pose a resource risk that the actual quantity of wind and solar irradiation can be less than expected. The resource risk imposes uncertainty in short-, medium- and long-term energy generation and consumption. Hence such risk needs to be actively considered and mitigated during the evaluation and operational phase of renewable or hybrid energy system projects. This paper provides a comprehensive review of renewable resource risk quantification techniques. Subsequently, a list of renewable energy resource risk quantification methods is discussed i.e., renewable reliability (i.e., the percentage of demand met by renewables), energy deficit and energy oversupply index, probability of exceedance (PoE) for annual energy production (AEP), probability of generating at least k MW of renewable power, capacity factor. Finally, some selected matrices are used to assess the effect of different risk mitigation options, e. g. the optimal size of energy storage.

Keywords: Mining, renewable resource risk, resource reliability, sustainable energy.

1. INTRODUCTION

Mining is one of the most energy-intensive industries. It accounts globally for 11% of the total final energy consumption and 38% of industrial final energy consumption (McLellan et al., 2012). Also, being one of the largest expenses in mining, energy on average accounts for 15% to 40% of the total operational cost (Igogo et al., 2020). Having said that, the sector's final energy consumption is still heavily dependent on fossil fuels, with 62% of final energy consumption being made up of oil, gas, and coal directly, while 35% is made up of electricity from the grid that often includes fossil fuels (Maennling and Toledano, 2018). With the increase in mineral demand, combined with declining ore grades, it is expected that the energy demands in mining will only grow in the future, potentially increasing its already large greenhouse gas (GHG) footprint (Nasirov and Agostini, 2018). Under these circumstances, the mining industry has been under enormous pressure to reduce its environmental impacts. This is leading to an increasing interest in adopting renewable energy to power mining operations. With increasing energy costs, renewable energy like solar and wind present a viable option not only to improve the environmental footprint but also to reduce overall costs with optimized operation of mines. While renewable energy generators i.e., solar photovoltaics (PV) and wind turbines have numerous benefits such as environmental friendliness, natural availability, and lower life-cycle cost; the major drawbacks are their temporal intermittency and seasonal and long-term variability. Therefore, renewable energy generators pose a resource reliability risk that can be manifested as a quantity risk—i.e., the risk that the quantity of wind and sunshine will be less than expected (Bolinger, 2017). The resource reliability risk imposes uncertainty in short-, medium- and long-term energy generation and consump-tion. Hence such risk needs to be actively considered and mitigated during the evaluation and development phase of renewable or hybrid energy system projects. There-fore, a methodology is required to quantify the energy supply risk in a renewable or hybrid energy generation system. Subsequently, such risk quantification method can be used to analyze the effect of different risk mitigation options, e. g. the optimal size of energy storage and/or backup/emergency energy generator or through grid or de-mand flexibility. In this paper, we have focused exclusively on battery energy storage as a risk mitigation option. Nevertheless, the methodology presented can be adapted to other mitigation strategies as well.

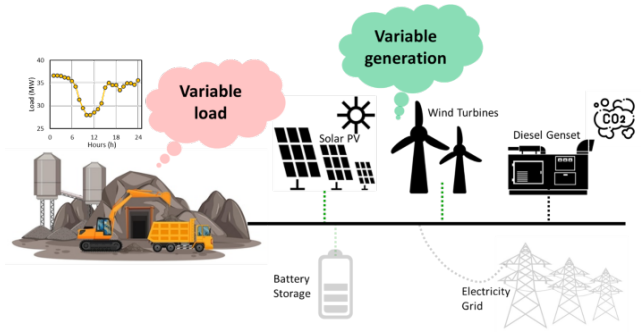

Fig. 1. Hybrid energy generation system for mines

2. MATERIALS AND METHODS

2.1 Hybrid Energy Generation System for Mines

A hybrid energy system combines multiple types of energy generators and/or backup energy sources like storage or grid in a complementary fashion to ensure dependable power supply at a competitive cost (Fathima and Palanisamy, 2015). One of the major benefits is that it can capitalize on existing grid infrastructure and add different components to help reduce costs, environmental impacts, and system disruptions. Hence, a hybrid energy system is a viable option that can help the mining industry to transition away from fossil fuel-based operations. Depending on the renewable resource availability and economic feasibility, a hybrid energy system for mines can consist of solar PV, wind turbine along with diesel generators (DG) and/or storage and grid as backup source, as shown in Fig. 1. Of course, the actual configuration will vary depending on site and mine-specific requirements. However, including solar and wind generators in mining energy generation systems comes with disadvantages like temporal intermittency, and seasonal and long-term variability. Traditional mining energy sources like diesel and grid can deliver energy whenever needed. Contrarily, solar and wind generators can only deliver energy when the sun is shining, and wind is blowing. This makes both the demand side and the generation side of the energy system variable. The challenge lies in the need to constantly balance energy demand with energy generation. Hence, backup sources like storage, diesel generators, or connection to regional electricity grids are essential for the security of supply. Due to the remote nature of mining sites, combining solar and wind energy with battery energy storage systems (BESS) is seen as the most viable option to initiate energy transition in the mining industry.

2.2 Wind Energy

The use of wind energy in electricity generation is widespread in today's world. Typically wind turbines, devices that convert the kinetic energy of wind into electrical energy, are used for this purpose. Wind energy can also be used to complement solar energy due to its availability during the night and on cloudy days.

Wind Resource Assessment

The economic value of wind energy generators depends on the availability of wind resources at the intended geographical location. Hence, the wind resource assessment is a crucial part of the feasibility study. Even though the approaches for resource assessment typically vary depending on many factors like purpose, stage of development, and generator types under consideration, such calculations are often based on some on-site wind measurement, sometimes augmented by meteorological modeling, and likely to be combined with longer-term measurements from offsite (but ideally nearby) reference stations. Typically, Weibull distribution is used to represent the frequency of wind speeds at a specific location. The general form of the Weibull distribution for wind speed takes the following form as shown in equation (1) as presented in (Al Buhairi, 2006),

$$f_v(v) = \frac{k}{c}\left(\frac{v}{c}\right)^{k-1} \exp\left[-\left(\frac{v}{c}\right)^{k}\right] \tag{1}$$

Wind Turbine Modelling

A model of a wind turbine is typically represented by a power curve, which is a plot between power output and wind speeds at a particular hub height. In this work, a piecewise model of a power curve from Devrim and Eryilmaz, 2021 is used as described in equation (2),

$$P_i(v) = \begin{cases} 0 & \text{if } v < v_{ci} \text{ or } v \geq v_{co} \\ 1 & \text{if } v_{ci} \leq v < v_r \\ P_r & \text{if } v_r \leq v < v_{co} \end{cases} \tag{2}$$

where v_{ci}, v_{co}, and v_r are cut-in, cut-off, and rated wind speeds respectively. P_r is the rated output power of the wind turbine.

Specification data for different wind turbines can be obtained freely from the wind turbine library maintained by Open Energy Platform.

2.3 Solar Energy

Solar energy is one of the fastest-growing renewable energy technologies available today. The most common options for utilizing solar energy are PV and solar thermal systems. In this paper, the focus will be on solar PV, which are electronic devices that convert sunlight directly into electricity.

Solar Resource Assessment

One of the major factors for the economic feasibility of solar PV systems is the availability of solar energy that can be utilized to produce electricity. Typically, solar irradiation, the amount of energy that reaches a unit area in a unit of time (expressed as Wh/m^2), is used to quantify available solar energy. There are different methods available to estimate solar irradiation in a given location such as based on in situ data, derived from satellite data, or a combination of both. Typically, Beta distribution is used to represent the solar irradiation data. The general form of the Beta distribution is depicted in equation (3) as described in Liu et al. (2016),

$$f(r) = \frac{\Gamma(\alpha+\beta)}{\Gamma(\alpha)\Gamma(\beta)}\left(\frac{r}{r_m}\right)^{\alpha-1}\left(1-\frac{v}{A}\right)^{\beta-1} \tag{3}$$

where r and r_m are the actual solar intensity and the maximum intensity in a time period, α and β are the shape parameters of Beta distribution, Γ is a function of Gamma.

Solar PV Modelling

The output power of solar PV is calculated from equation (4),

$$P_{PV} = \eta_{PV} A_{PV} PR_{PV} \times GHI \tag{4}$$

where, η_{PV}, A_{PV}, PR_{PV} and GHI denotes solar module yield, area, performance ratio (also known as a coefficient for losses that range between 0.9 and 0.5, the default value is 0.75), and global horizontal irradiance. It's worth noting that the above formula is an estimation, as the actual solar power generation depends on many factors such as temperature, shading, dust, and the age of the panel. Some of these factors can be covered by solar module yield.

2.4 BESS

BESS plays an important role in renewable energy integration due to its ability to directly address intermittency issues that are inherent to renewable energies. Major benefits of BESS include assistance in peak shaving, load shifting, voltage and frequency regulation by adding virtual spinning reserve, etc. Typically, a BESS consists of battery cells connected in parallel and series configurations with inverters to facilitate charging and discharging.

BESS Modelling

A simplified battery model based on charge quantity and state of charge (SoC) calculation is used in this work. The charge quantity of battery storage at the time t is calculated by equation (5) according to Deshmukh and Deshmukh (2008),

$$E_B(t) = E_B(t-1)(1-\sigma) + \left(E_{GA}(t) - \frac{E_L(t)}{\eta_{inv}} \right) \times \eta_{bat} \tag{5}$$

where, $E_B(t)$ and $E_B(t-1)$ are the charge quantities of battery storage at the time t and $(t-1)$, σ is the hourly self-discharge rate, $E_{GA}(t)$ is the total energy generated by the energy source after energy loss in the controller, $E_L(t)$ is load demand at the time t, η_{inv} and η_{bat} are the efficiency of inverter and charge efficiency of battery storage. The charge quantity of battery storage is subject to the constraints represented by equation (6),

$$E_{Bmin} \leq E_B(t) \leq E_{Bmax} \tag{6}$$

where E_{Bmax} and E_{Bmin} are the maximum and minimum charge quantity of battery storage.

When referring to BESS, it is more common to use an empirical definition of SoC, as represented in equation (7),

$$SoC = \frac{E_B(t)}{E_{Bmax}} \tag{7}$$

2.5 Renewable Resource Risk

Often the availability of renewable resources dictates the economic viability of renewable energy integration. Hence, a feasibility study for renewable energy projects must include resource assessment as a first step. Most often a "$P50$" estimate of wind speed or solar irradiance is used to calculate the annual energy production that forms the basis for economic calculation. This introduces two primary sources of potential error or bias: 1) the systematic bias from the resource measurement and/or modeling techniques used and 2) the random error related to the inherent short-, medium- and long-term variability of the resource over time. There is a third error of systemic type from energy converter models that are used to estimate the amount of energy generation. Another aspect that is often overlooked in such traditional approaches to the feasibility study is that during the operational phase, the energy demand must always be matched by the energy available instead of ensuring only an annual balance. This means energy must be balanced in short-terms like 15− minutes, hourly, etc., and medium-terms like daily, weekly, monthly, etc. to long-term like yearly and over the project lifetime. Thus, the traditional methods overlook the dynamic energy supply risk and are unable to analyze and provide risk mitigation options and their associated costs. In addition to this, for completeness, such a feasibility study should also consider options related to the other side of the energy balancing act i.e., the demand side flexibility options. Energy consumption peaks should be avoided to reduce the risk of emergency shutdowns and high peak price payments. At least, the decision makers need ways/tools to compare different risk mitigation alternatives related to both the supply- and demand-side that also include associated costs of corresponding options. For example, what are the overall costs and benefits of reducing peak energy demand at rear times with no or exceptionally low renewable generation against installing additional energy storage or emergency backup generators to cover rear peaks? There is a need for a well-defined method/tool to quantify, predict, and reduce the operational risks of energy supply and to evaluate means to reduce these risks.

There are multiple approaches used in the literature to quantify the renewable resource risk. The most common ways to quantify the renewable resource risk are:

- Probability of exceedance (PoE) for annual energy production (AEP).
- Renewable reliability (i.e., the percentage of demand met by renewables).
- Probability of generating at least k MW of renewable power.
- Energy deficit index and energy oversupply index
- Capacity factor

One of the most widely used matrices is the probability of exceedance for annual energy production (illustrated in Fig. 2(a), which, with just a few key inputs, can be used to estimate the probability that, for example, the wind or solar generation at a given site will fall below a given level (Bolinger, 2017). This also allows comparison of the resource risk among multiple project sites in terms of probabilistic values. Probability of exceedance is often represented as "$P-level$" which ranges from P 1 (i.e., there

is only a 1% chance that actual generation will exceed the $P1$ estimate) to $P99$ (i.e., there is a 99% chance that actual generation will exceed the $P99$ estimate). In comparison to the central or median estimate that is equivalent to the "$P50$" estimate, the probability of exceedance allows the project analyst to choose different "$P-level$" for wind and/or solar generation. Another common way to quantify the renewable resource risk is by calculating the reliability (i.e., the percentage of demand met by renewables) (Tong et al., 2021). Devrim and Eryilmaz (2021) proposed calculating the probability of generating at least k kW of renewable power. Additionally, simple indicators like the energy deficit index, energy over-supply index, and capacity factor can be calculated to quantify energy supply risk.

According to Tong et al. (2021), the renewable energy system's reliability index is the percentage of the total load that is met by renewables at a given time, as depicted in equation (8),

$$I_{reliability} = \frac{\text{Renewable generation at time t}}{\text{Load at time t}} \times 100\% \quad (8)$$

The energy deficit index is defined as the ratio between energy shortage and energy demand in a particular hour, as described in equation (9),

$$I_{\text{deficit}} = \frac{\text{Energy deficit at time t}}{\text{Load at time t}} \times 100\% \quad (9)$$

Similarly, the energy oversupply index is the ratio between energy oversupply and energy demand in a particular hour, as shown in equation (10),

$$I_{\text{oversupply}} = \frac{\text{Energy over supply at time t}}{\text{Load at time t}} \times 100\% \quad (10)$$

The capacity factor of a renewable energy system is a measure of how much electricity the system generates compared to its maximum potential output. It is calculated by dividing the actual energy generated by the system over a certain period of time by the maximum possible energy that could have been generated during that same period (Ahmad et al., 2018). The result is then expressed as a percentage. The formula for calculating the capacity factor can be expressed as below,

$$C_F = \frac{\text{Actual energy generated at time t}}{\text{Maximum possible energy generation}} \times 100\% \quad (11)$$

2.6 Renewable Resource Data

There are several ways to obtain solar and wind resource data for a specific location. The historical wind data can be obtained from various sources such as the National Renewable Energy Laboratory (NREL) or other national meteorological services. These datasets usually provide data in the form of wind speed and direction measurements at a specific location and time. Some of these datasets can be downloaded in bulk, while others require you to request access or download data on a case-by-case basis. Similarly, the historical solar radiation data can be

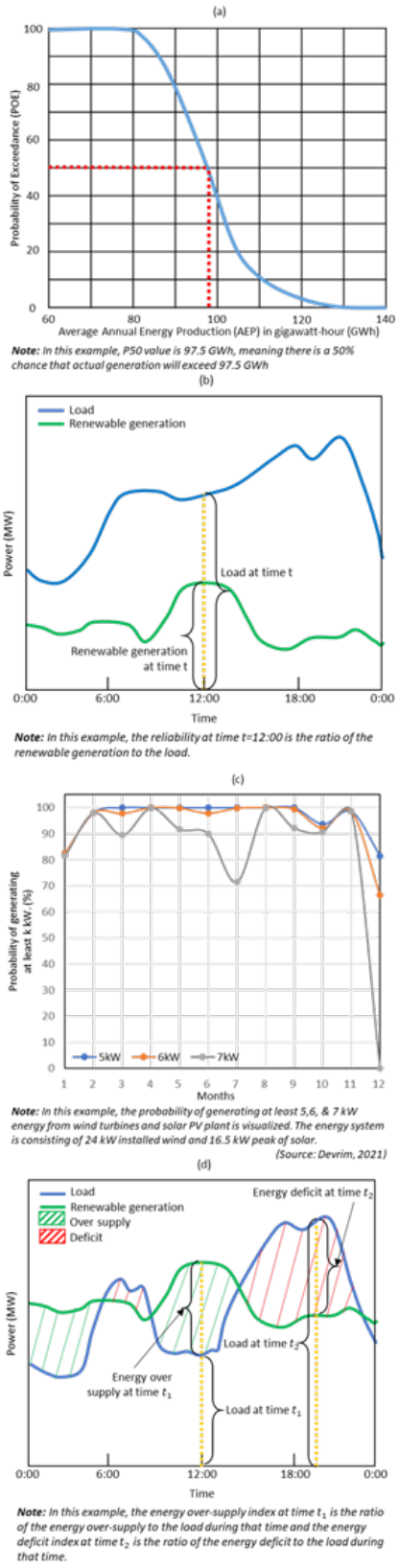

Fig. 2. Illustration of (a) probability of exceedance, (b) reliability (% of load met by renewables), (c) probability of generating at least k kW of renewable power, and (d) energy deficit and oversupply index, are visualized.

obtained from various sources such as NASA's Surface Meteorology and Solar Energy (SSE) dataset, the NREL or other sources. These datasets usually provide data in the form of solar radiation measurements (usually in kWh/m^2 or W/m^2) at a specific location and time. Some other online databases and platforms provide solar and wind data, such as the European Renewable Energy Data Platform (EURODATA) and Renewable Resource Data Center (RReDC). It's important to note that using historical data alone may not provide a complete picture of the renewable energy resources available in a specific location, and it's recommended to combine with other sources of information, such as on-site measurements, local weather patterns, topography, and land use, etc. to get a more accurate assessment.

In this work, NASA's Solar and meteorological resource data- "POWER data" are used for wind and solar resource assessment (NASA, 2024). This satellite and modeled-based database are accurate enough to provide reliable solar and meteorological resource data over regions where surface measurements are sparse or non-existent and offer two unique features – the data are global and contiguous in time (Pavlović et al., 2013). Microgrid design tools such as HOMER and RETscreen also use "Power data" as one of the data sources. Most importantly, the data from "POWER data" is available at multiple temporal levels: hourly, daily, and monthly.

For this work, the hourly data for wind speed, GHI, atmospheric temperature, and pressures are collected over 21 years from 2001 to 2021 for a location in Scotland (Latitude: 57.0161 and Longitude: -2.8719; referred to as location-1). To get an overview of the data, wind speed, and solar irradiation are visualized in Figs. 3 and 4. The wind speed shows greater variability with a mean around 7.4 m/s. Interestingly, for the selected location the wind speed is slightly higher in winter than summer. This is linked to the fact that the winter brings higher temperature gradients. On the other hand, as expected the solar irradiation peaks during summer and very low during winter.

3. RESULT AND DISCUSSION

3.1 Prerequisites

To estimate power generation from available wind and solar resources, the wind turbine model described in Section 4.2 and the solar PV model described in Section 5.2 are used. The hourly electricity generation from wind and solar is calculated for the entire historical dataset of 21 years. The wind and solar park are sized such that it can on average meet 20% of the load assumed to be 20 MW. In reality, the load will be variable but for the sake of simplicity, it is assumed to be constant here. Eventually, six different cases as presented in table 1 are formulated by considering different shares of solar and wind in the renewable energy share. The wind turbine and solar module specifications presented in table 2 and 3 are used for the calculation. Accordingly, the wind farm and solar park capacities are upscaled to fulfill the installed power needed for each use case.

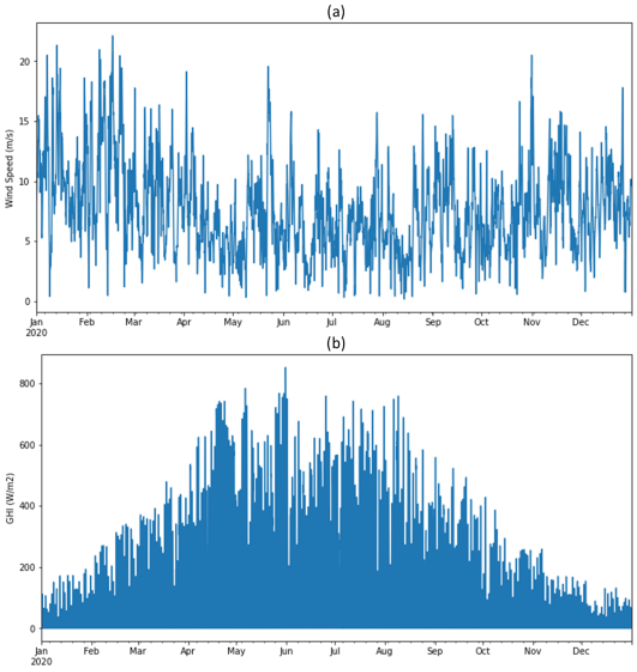

Fig. 3. Hourly (a) wind speed and (b) solar irradiation for the year 2020.

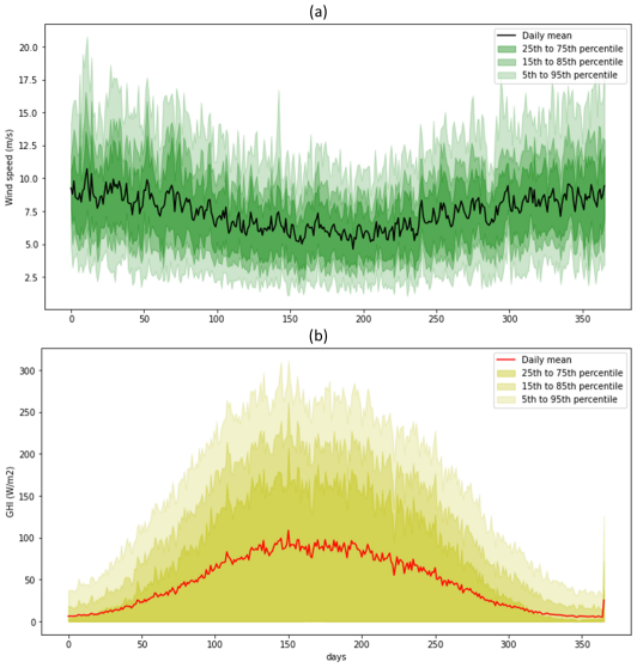

Fig. 4. Hourly (a) wind speed and (b) solar irradiation for the year 2011-2020.

3.2 Renewable Resource Reliability

In Figure 11 the wind and solar energy generation corresponding to the historical dataset for a given location is visualized. To be able to include both wind and solar energy case-2 was selected. As expected, the energy generation from wind and solar follows the same trend as available wind and solar resources. However, the variability of available energy is something to note here. If we look at the hourly mean as well as percentile values, wind has

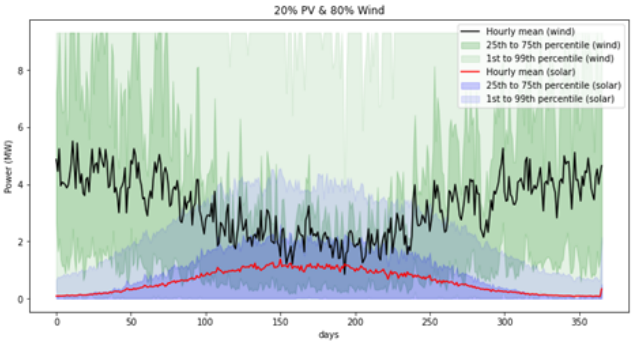

Fig. 5. Individual power generation from wind and solar plant for case 2.

much larger variability than solar. Of course, the wind speed variation is partly amplified due to the high share of wind in case-2. However, variability in wind energy generation comes from high wind speed variability. One interesting fact is that wind generation cannot be more than the total rated power of the wind park that is imposed by the cumulative power curves. Another observation is that over a year solar and wind can act as complementary energy sources for this location. By using both solar and wind energy together, it is possible to reduce the impact of the yearly variability of each source and have a more consistent supply of electricity.

Subsequently, the total energy produced combined by the wind and solar is calculated by adding individual generation. The cumulative power generation for each of the cases is chronologically visualized in Fig. 6. By looking at the average energy generated by each of the system configurations, it is obvious that case-2 and case-3 provide fairly stable average energy throughout the year. The results are summarized in table 4. For better visualization, the mean reliability for different cases is plotted in Fig. 7. The mean reliability decreases as the system configuration changes from "Case-1: 0% PV and 100% wind" to "Case-6: 100% PV 0% wind". Meaning, for this specific location wind wind-heavy systems offer higher mean reliability. On the other hand, the mean energy deficit and the oversupply index increase with solar-heavy systems. However, one must not get deceived by the facts or base their conclusion entirely by looking at the mean values only. The local variation must be considered as well. Mean value over such a long timescale often doesn't tell the whole story.

Table 1. Cases with different share of solar and wind

Case no.	Description
Case-1:	0% PV & 100% Wind
Case-2:	20% PV & 80% Wind
Case-3:	40% PV & 60% Wind
Case-4:	60% PV & 40% Wind
Case-5:	80% PV & 20% Wind
Case-6:	100% PV & 0% Wind

Table 2. WT (Enercon e-53/800) specification

Parameter	Value	Unit
Rated power:	810.0	[kW]
Cut-in wind speed:	3.0	[m/s]
Rated wind speed:	12.0	[m/s]
Cut-out wind speed:	26.0	[m/s]
Rotor Diameter:	52.9	[m]
Hub height:	60/73	[m]
Swept area:	2198	[m^2]

Table 3. PV module specification

Parameter	Value	Unit
Module efficiency:	15	[%]
Performance ratio:	0.75	[-]
Life:	25	[years]

Table 4. Renewable Reliability at location-1 for different cases

Case	Mean reliability	Mean P50 reliability	Mean energy deficit index	Mean oversupply index
1	19.8%	12.5%	12.5%	21.9%
2	19.2%	14.2%	10.8%	17.0%
3	18.5%	14.6%	10.8%	17.0%
4	17.9%	12.8%	11.3%	16.4%
5	17.3%	9.1%	11.7%	25.3%
6	16.6%	1.2%	14.5%	32.0%

Subsequently, the same calculation is performed for another location in central Australia (Latitude: -22.5909 and Longitude: 133.4432, referred to as location-2). As can be seen from table 5 and Fig. 8, the trends are reversed as this location has relatively higher solar irradiation and lower wind. This shows how renewable generation and their reliability can be very much location-dependent and thus the system configuration will vary based on renewable resource availability.

Table 5. Renewable Reliability at location-2 for different cases

Case	Mean reliability	Mean P50 reliability	Mean energy deficit index	Mean oversupply index
1	14.5%	12.0%	8.7%	11.5%
2	19.8%	17.9%	9.2%	11.6%
3	25.1%	16.6%	14.2%	24.4%
4	30.4%	12.7%	21.5%	37.6%
5	35.7%	12.7%	21.5%	50.6%
6	41.1%	2.2%	37.1%	63.8%

3.3 PoE for AEP

Once the preferred share of wind and solar for a specific location is known, the AEP of the system is calculated at different PoE levels. To do so, individual AEP with PoE for wind and solar PV is computed for location-1. For a fair comparison between wind and solar case-3 with 60% wind and 40% solar is selected for this analysis. For wind, the spread between $P99$ and $P1$ for AEP is around 19.5 GWh to 34.5 GWh. Subsequently, the spread between $P99$ and $P1$ for AEP is around 10.6 GWh to 12.8 GWh for solar park. For a combined system, the AEP values are just added together as presented in Fig. 9. Now, this graph can be used as the basis of financial calculation when a $P-value$ is given. As mentioned earlier, typically a $P50$ AEP is used for such calculation. For a more conservative calculation, a higher $P-value$ can be used.

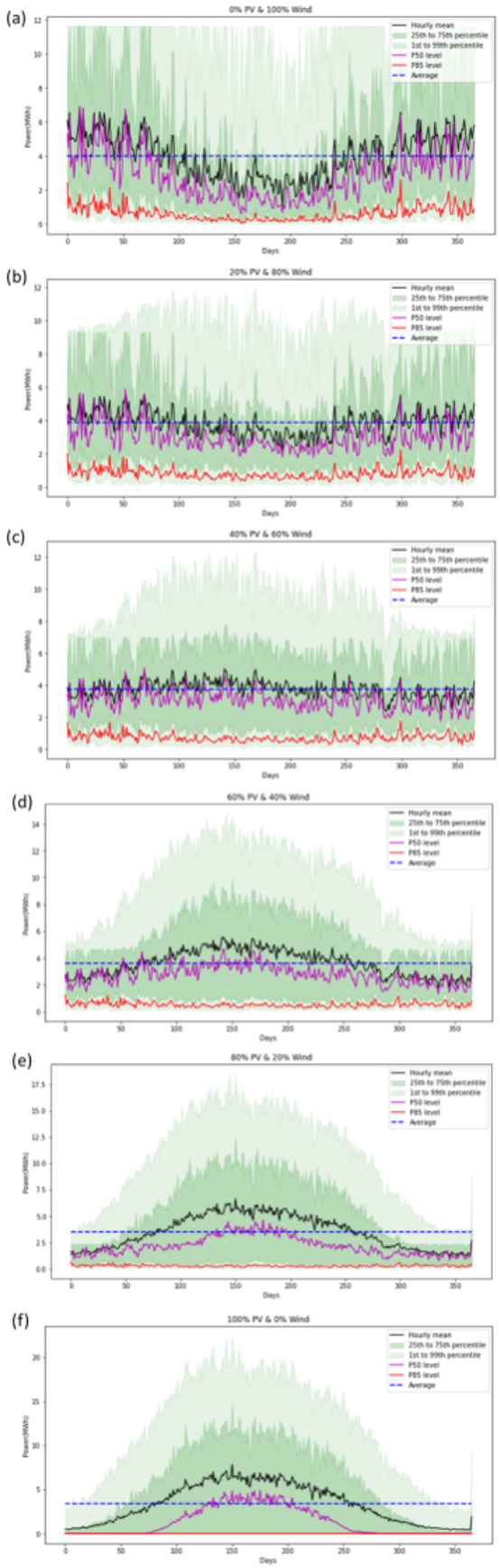

Fig. 6. Combined power generation from wind and solar plant for different cases.

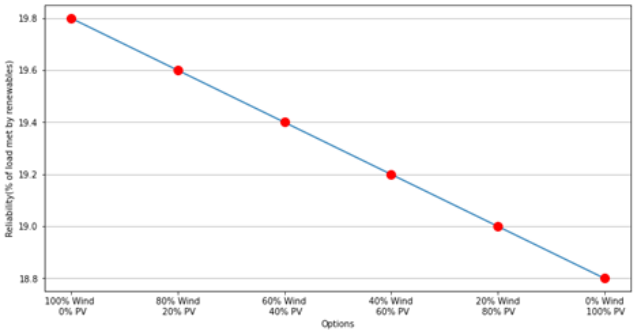

Fig. 7. Renewable reliability of different cases for a location-1.

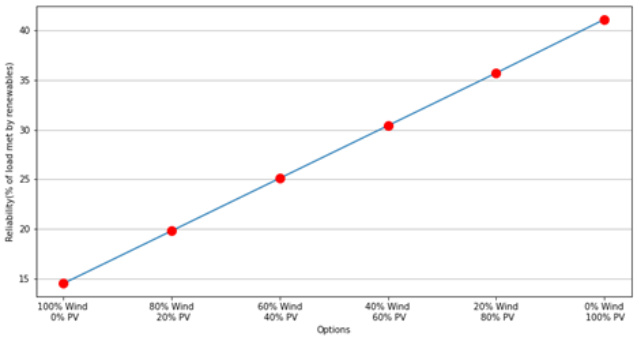

Fig. 8. Renewable reliability of different cases for a location-2.

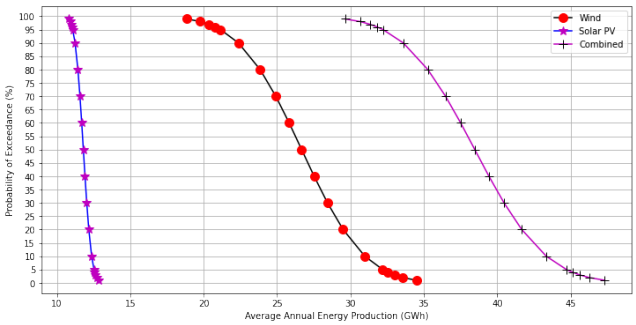

Fig. 9. AEP with PoE for case-3 at location-1.

3.4 Renewable Risk Mitigation with BESS

To get a further understanding of renewable energy variability, the energy deficit (or power shortage) and oversupply for case-3 over a year is visualized in Figs. 23 to 25. It is important to note here, a constant load is considered to calculate the energy deficit and the oversupply.

Fig. 10(a) shows, that the energy deficit and oversupply are spread out over the entire year except for some parts, which is preferable when considering a BESS. While analyzing the monthly trends, it was found that there are months where the energy deficit and oversupply are equally distributed (as in Fig. 10(b) and months where that is not the case (Fig. 10(c). The argument here is that a BESS needs to be designed to cover a month where the renewable generation was particularly low. In that case, the BESS needs to be oversized and that is associated with high capital cost.

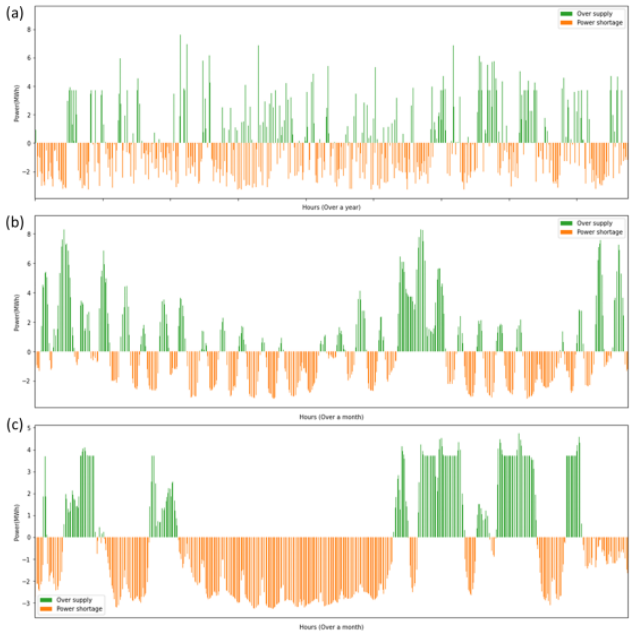

Fig. 10. Energy deficit and oversupply for (a) 2001, (b) June 2001, and (c)December 2001, (case-3, location-1)

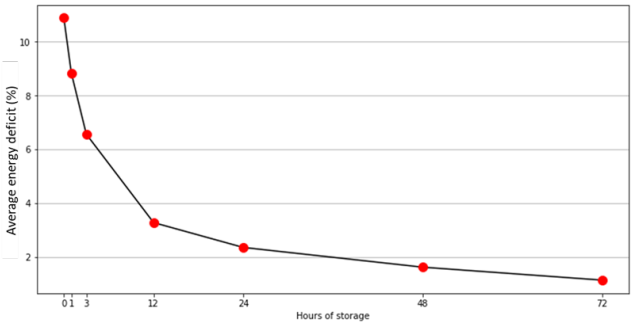

Fig. 11. Average energy deficit index for BESS with Solar and Wind system (case-3, location-1)

To analyze how the BESS can help mitigate some of the variability introduced by renewable energy, the BESS model described earlier is used. Subsequently, different battery size is used to calculate the corresponding average energy deficit index for systems with BESS, solar and wind (case-3). The results are visualized in Fig. 11 where the BESS capacities are represented as hours of storage. Here, "1 hour of storage" corresponds to a BESS size that can cover the entire load by an hour. As can be seen from Fig. 11, initially the average energy deficit index reduces sharply with increasing battery sizes. The slope of the curve diminishes as the BESS size increases.

To analyze how different shares of solar and wind change the energy deficit versus the BESS size graph, the calculations are repeated for different cases (case-1 to case-6). The result is summarized in Fig. 12. "Case-2: 20% PV and 80% wind" can have a lower energy deficit index than "case-1: 0% PV and 100% wind". Interestingly, with further increase in PV share in the system results in a higher energy deficit index. Overall, the case-2 with BESS can provide the lowest energy deficit index.

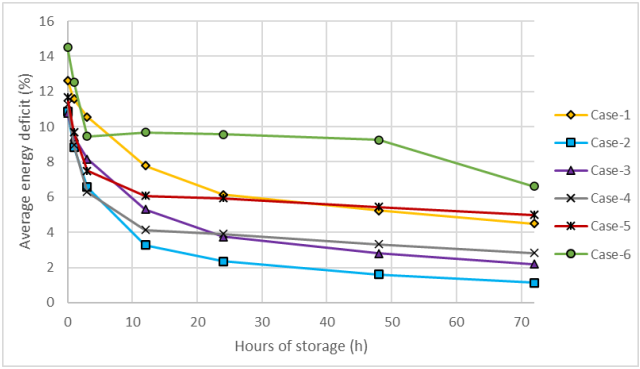

Fig. 12. Average energy deficit index for BESS with Solar and Wind system (case-1 to 6, location-1)

4. CONCLUSIONS

The mining industry has huge potential for renewable energy to meet its energy needs while reducing environmental footprint and overall cost. Freely available solar and meteorological data sources provide a good starting point for the assessment of renewable energy potential, allowing for a fairly accurate and efficient evaluation of the feasibility of different renewable energy projects for mines. These datasets can provide information on factors such as solar radiation levels, wind speeds, and temperature, which are all important for determining the potential output of renewable energy systems. Indeed, the renewable energy generation potential of mines will vary depending on the onsite availability of renewable resources. Accordingly, the preferred share of different renewable sources, here solar and wind, in a mining energy grid will differ significantly at different sites. The reliability of renewable energy generation from the same solar-wind combination can be utterly different in different locations. Interestingly, the reliability trend can reverse for two different locations, meaning increasing the share of solar in a wind-solar mix can result in both decreasing or increasing reliability based on the location. Additionally, using both solar and wind energy together, it is possible to reduce the impact of yearly variability of each source and have a more consistent supply of energy. For financial calculation, annual energy production with the probability of exceedance can act as a better indicator. When it comes to the battery energy storage sizing, the benefit diminishes with increasing size. Meaning, the reduction in overall energy deficit from a solar-wind-battery system decreases exponentially with increasing battery energy storage size. Additionally, the lowest possible energy deficit is also heavily dependent on the share of solar and wind in the system.

REFERENCES

Ahmad, J., Imran, M., Khalid, A., Iqbal, W., Ashraf, S.R., Adnan, M., Ali, S.F., and Khokhar, K.S. (2018). Techno economic analysis of a wind-photovoltaic-biomass hybrid renewable energy system for rural electrification: A case study of Kallar Kahar. *Energy*, 148, 208–234. doi:10.1016/j.energy.2018.01.133.

Al Buhairi, M.H. (2006). A statistical analysis of wind speed data and an assessment of wind energy potential

in Taiz-Yemen. *Ass. Univ. Bull. Environ. Res*, 9(2), 21–33.

Bolinger, M. (2017). Using probability of exceedance to compare the resource risk of renewable and gas-fired generation. Technical report.

Deshmukh, M.K. and Deshmukh, S.S. (2008). Modeling of hybrid renewable energy systems. *Renew. Sustain. Energy Rev.*, 12(1), 235–249. doi: 10.1016/j.rser.2006.07.011.

Devrim, Y. and Eryilmaz, S. (2021). Reliability-based evaluation of hybrid wind–solar energy system. *Proc. Inst. Mech. Eng. Part O J. Risk Reliab.*, 235(1), 136–143.

Fathima, A.H. and Palanisamy, K. (2015). Optimization in microgrids with hybrid energy systems – A review. *Renew. Sustain. Energy Rev.*, 45, 431–446. doi: 10.1016/j.rser.2015.01.059.

Igogo, T., Lowder, T., Engel-Cox, J., Awuah-Offei, K., and Newman, A.M. (2020). Integrating Clean Energy in Mining Operations: Opportunities. *Challenges, Enabling Approaches (No. NREL/TP-6A50-76156)*, 43.

Liu, Z., Liu, W.l., Su, G.c., Yang, H., and Hu, G. (2016). Wind-solar micro grid reliability evaluation based on sequential Monte Carlo. In *2016 Int. Conf. Probabilistic Methods Appl. to Power Syst.*, 1–6. doi: 10.1109/PMAPS.2016.7764073.

Maennling, N. and Toledano, P. (2018). The renewable power of the mine. *Available SSRN 3661616*. doi: 10.2139/ssrn.3661616.

McLellan, B.C., Corder, G.D., Giurco, D.P., and Ishihara, K.N. (2012). Renewable energy in the minerals industry: a review of global potential. *J. Clean. Prod.*, 32, 32–44.

NASA (2024). https://power.larc.nasa.gov/.

Nasirov, S. and Agostini, C.A. (2018). Mining experts' perspectives on the determinants of solar technologies adoption in the Chilean mining industry. *Renew. Sustain. Energy Rev.*, 95, 194–202. doi: 10.1016/j.rser.2018.07.038.

Open Energy Platform (2024). https://openenergy-platform.org.

Pavlović, T.M., Milosavljević, D.D., and Pirsl, D.S. (2013). Simulation of photovoltaic systems electricity generation using homer software in specific locations in Serbia. *Therm. Sci.*, 17(2), 333–347.

Tong, D., Farnham, D.J., Duan, L., Zhang, Q., Lewis, N.S., Caldeira, K., and Davis, S.J. (2021). Geophysical constraints on the reliability of solar and wind power worldwide. *Nat. Commun.*, 12(1), 1–12.